Chapter 1-8

# Microfabric Studies as Indicators of Deformation Mechanisms and Flow Laws Operative in Mountain Building

S.M. Schmid

*Geologisches Institut ETH,*
*Zürich, Switzerland*

## Abstract

After an introduction into the major deformation mechanisms the following applications to tectonic studies are discussed:
(i) Paleostress estimates based on the extrapolation of experimentally determined flow laws and based on the size of dynamically recrystallized grains; (ii) the significance of crystallographic preferred orientation work; and (iii) mechanisms of strain softening leading to localized deformation in shear zones.

## I. Introduction

In discussions with field oriented geologists an experimental geologist sometimes notes criticism with regard to the applicability of the results of experimental rock deformation to the study of naturally deformed rocks. The critics often point out that the experiments were performed under such simple conditions (co-axial strain path, constant stress or strain rate, homogeneous monomineralic rocks) that they are inadequate to throw light on the more complex processes in natural environments. However, any laboratory study must begin with well defined boundary conditions so that the influence of a great number of variables on rock creep can be recognized. Also it is necessary to learn as much as possible about the physics and the mechanisms of rock deformation in order to avoid erroneous extrapolations from the laboratory into the geological situation.

It is the study of the microfabric in both experimentally and naturally deformed rocks which permits direct comparisons to be made between nature and experiment. The microfabric records the active mechanisms of deformation and its study therefore helps to close the gap between experiment and field observation.

Some of the complexities of natural tectonic situations can be modelled much more easily by using analytical or numerical methods or by using readily deformable analogue materials than by an attempt to perform more complex experiments on natural rock specimens. In this case it is important however to know as much as possible about the rheology of rocks which depends on the active deformation mechanisms recorded in the microfabric.

This contribution will specifically discuss some selected applications to tectonic studies. Thereby some of the goals of microfabric studies are illustrated within the framework of tectonic studies in general. In order to do so it was felt necessary first to introduce the non-specialist reader into some basic concepts of flow laws and deformation mechanisms.

## II. Some General Remarks on Flow and Deformation Mechanisms

A rock loaded under a constant differential stress $\sigma$ (classical creep test) will immediately shorten elastically. Later it will undergo a permanent change of shape at a strain rate $\dot{e} = \mathrm{d}e/\mathrm{d}t$ which is dictated primarily by three factors according to a flow law of the general form:

$$\dot{e} = \dot{e}\ (\sigma, e, T)$$

where the stress difference $\sigma$ $(= \sigma_1 - \sigma_3)$ (informally referred to as "stress"), the strain $e$ and the temperature $T$ are the most important quantities determining the resulting strain rate. Strictly, such a flow law is only valid as long as other factors such as confining pressure, water content or partial pressure, grain size etc. are held constant or can be assumed to have no major influence on the rheological properties.

Confining pressure is usually assumed to be of minor importance in the ductile field, once frictional processes (cataclasis) can be ruled out (Paterson, 1978). Water can have a "mechanical" effect through the well known pore pressure effect (Hubbert and Rubey, 1959), again in the brittle and cataclastic fields, or it may have an influence on the nature of atomic bonding in silicates, influencing the resistance to deformation by crystal plasticity, a phenomen known as hydrolitic weakening (Griggs, 1967). In the latter case there is evidence that pressure enhances the solubility of water in quartz and therefore, that pressure strongly influences the rock strength outside the cataclastic field as well (Tullis *et al.*, 1979; Paterson and Kekulawala, 1979). The influence of grain size will be discussed in more detail in the next section.

During the first stages of deformation the strain rate strongly depends on strain (primary creep); after a few percent strain the rate of deformation usually decreases to a constant value. The rock is then said to deform in steady state. Ideally, strain has no influence on the strain rate any more. We will see later that rocks may eventually soften at high strains causing the strain rate to increase again. At this point it is important to say that the concept of steady state is used here to merely imply flow at constant stress and strain rate.

In the case of a constant strain rate experiment the stress may rise with increasing strain (strain hardening), it may stay constant (steady state) thereafter, or it may eventually decrease with increasing strain (strain softening).

For thermally activated creep one can empirically derive flow laws from a series of experiments on the same rock, valid for steady state flow only. They are usually presented in the form of:

$$\dot{e} = \dot{e}_0 \exp -H/RT \; f(\sigma) \qquad (1)$$

where $\dot{e}_0$ is a material dependent constant, $H$ is the apparent activation energy for creep and $R$ is the Gas Constant. The stress dependence can adequately be described in most cases by either:

$$f(\sigma) = \exp \sigma/\sigma_0 \quad \text{(exponential creep law)} \qquad (2)$$

or

$$f(\sigma) = \sigma^n \quad \text{(power creep law)} \qquad (3)$$

where the constants $\sigma_0$ and $n$ determine the stress sensitivity of the strain rate. Because in most cases the parameter $n$ is found to be greater than unity, rocks usually deviate from linear viscous behaviour.

There is no single flow law for all conditions of stress and temperature, simply because the deformation mechanism is a function of stress and temperature as well. Associated with each of these deformation mechanisms is a different flow law. It is usual to subdivide the stress-temperature space into different fields by means of a deformation mechanism map (Ashby and Verrall, 1978 and Fig. 1). Within each of these fields a particular mechanism is dominant.

Such deformation mechanism maps are normally calculated from first principles by assuming specific microdynamical models. Experiments often merely provide numbers for the various material dependent constants in the theoretical flow laws.

The primary aim of these deformation mechanism maps is to outline the expected conditions of appearance of given deformation mechanisms outside the range of $\dot{e}$–$\sigma$–$T$–conditions accessible to the experimentalist. The main problem in the application of the laboratory data is the enormous gap between geological strain rates of the order of $10^{-10}s^{-1}$ to $10^{-15}s^{-1}$ (involving time spans of between 30 and 3 million years for 10% shortening strain) and the laboratory strain rates usually between $10^{-2}$ and $10^{-7}s^{-1}$. As can be seen in Fig. 1 one has a high chance of crossing a boundary between deformation mechanism fields by extrapolating down to lower strain rates and consequently to lower stresses at any given temperature. Therefore a flow law observed at high stresses under laboratory strain rates can only be extrapolated over a limited range of strain rates and stresses. In order to explore the flow behaviour at low stresses the experimentalist is forced to elevate the temperature beyond the range of temperatures expected under natural conditions

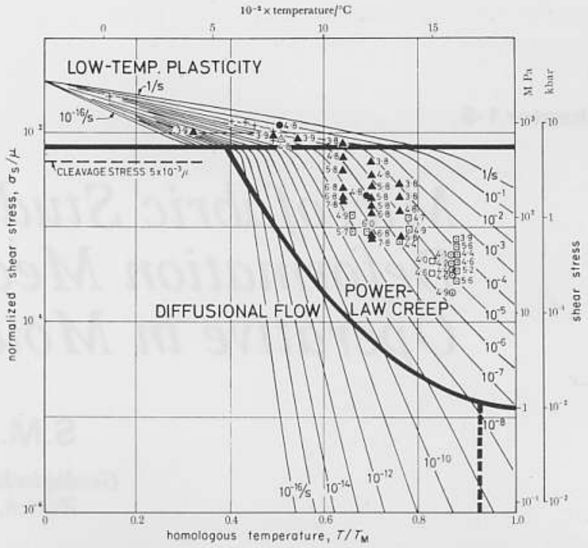


Fig. 1 Deformation mechanism map for olivine, taken from Ashby and Verrall (1978, Fig. 14). The map is constructed for a grain size of 100 μm and for zero confining pressure. The solid lines delineate deformation mechanism boundaries, superimposed are the constant strain rate contours. The various symbols indicate the position of experimental data on this map.

(Paterson, 1976). Thus, elevated temperatures are essentially used as a "trade off" for unattainably slow geological strain rates. Once a flow law has been established at high temperatures and low stresses the geologist has to extrapolate down to lower temperatures, along a path which is less likely to cross deformation mechanism boundaries.

There are some problems with the concept of steady state creep and the associated concept of flow laws and deformation mechanisms:

(i) Strain may alter the microstructure and this in turn causes strain hardening or strain softening (see section VI). In these cases the situation can no longer be described in terms of a single deformation mechanism map which assumes constant microstructure and steady state creep.

(ii) As will be discussed in the next section, there is a subtle difference between the deformation mechanism accounting for all or most of the total strain in the rock and the concept of a rate controlling step which contributes only a small part of the total strain (such as dislocation climb in power law creep).

(iii) Strictly a deformation mechanism map only applies to a particular mineral in a rock and it is rather difficult to talk about the deformation mechanism of a polymineralic rock. Many mylonites offer good examples for crystal plastic flow accompanied with recrystallization within quartz domains while the feldspars deform by cataclastic processes.

With these general remarks in mind we shall now review the major modes of deformation more specifically. This will allow us to discuss some geological applications such as paleostress estimates, crystallographic preferred orientation work and finally strain softening mechanisms.

## III. Deformation Regimes

Different approaches towards the problem of deformation mechanisms are possible. The physicist wants to be very exact about the processes on an atomic level and it is possible to theoretically postulate specific microdynamical models. There is a great number of such models and for a comprehensive review the reader is referred to Poirier (1976).

Here we will follow a more empirical approach. The experimentalist often derives empirical flow laws from a series of experiments and it is rarely clear what the exact mechanisms of deformation are. In such cases it is useful to talk about deformation regimes, defined by empirical flow laws and associated diagnostic microstructural imprints.

## A. Cataclastic Flow

The term "cataclastic" refers to a mode of deformation where fracture and subsequent loss of cohesion may occur on all scales. The brittle-ductile transition does not necessarily coincide with the transition from cataclastic to non-cataclastic processes. If intra- and intergranular fracture occurs along a dispersed network of microcracks, the bulk deformation of the rock may still be ductile in the sense that considerable amounts of permanent strain can be taken up without the typical stress drop associated with localized faulting, characteristic for the brittle field (Paterson, 1969).

Cataclastic flow is made possible by rolling and sliding of grains and crystal fragments of a cataclastically granulated rock. Since frictional resistance between the fragments depends on the magnitude of normal stress across cohesionless surfaces, this mechanism is strongly dependent on confining pressure and, in the presence of fluids, on the effective pressure, i.e. the difference between lithostatic and fluid pressure (Hubbert and Rubey, 1959).

Because to a first approximation deformation by cataclastic flow is not thermally activated, temperature and strain rate have little influence on the strength of the rock.

Figure 2 illustrates the microstructure typical for cataclastic flow within an experimentally produced fracture zone: grain size reduction by cataclastic processes produces a wide spectrum of angular fragments with a wide range of grain sizes. This type of grain size reduction should not be confused with the mechanism of grain size reduction by dynamic recrystallization, typical for mylonites (White *et al.*, 1980). Since the pioneering work of Carter *et al.* (1964) it is clear that mortar quartz in mylonites is the product of dynamic recrystallization during power law creep and that mylonites should not be referred to as cataclastic rocks (Higgins, 1971).

At more elevated temperatures and pressures crystal plastic deformation will successfully compete with fracturing because elevated temperatures promote the ease of glide within crystals and because higher pressures prohibit cataclastic processes associated with volume increases and frictional processes.

## B. Low Temperature Plasticity

Within this regime strain in the rock is largely achieved by the conservative motion of dislocations through the crystal lattice (i.e. the dislocations propagate strictly within crystallographic planes), or, on a larger scale of observation, by glide on slip systems defined by slip plane and direction. The resistance to glide is not controlled by friction and thus independent of confining pressure. There is a resistance to glide caused by either the necessity of breaking atomic bonds as a dislocation moves or by obstacles such as impurities, other dislocations or grain boundaries (lattice resistance versus obstacle controlled plasticity, Ashby and Verrall, 1978).

The resistance to dislocation glide is the rate controlling factor during deformation and usually an exponential stress dependence of strain rate (equation 2) is observed. The motion of dislocations is thermally activated, the apparent activation energy for creep is usually smaller than for the lattice self-diffusion. Thus, stress, temperature and strain rate become interrelated in the form of a pseudoviscous flow law (Fig. 1).

The fact that grain boundaries are obstacles to the free propagation of slip (and twinning in the case of calcite) into the neighbouring grain is reflected by the observation that the yield stress of fine-grained materials is generally higher than that of coarse-grained materials. This grain size depen-


Fig. 2 Grain size reduction by fracturing within a shear fracture zone in experimentally deformed quartzite. Note the angular shape and the wide spectrum of grain sizes of the crystal fragments.

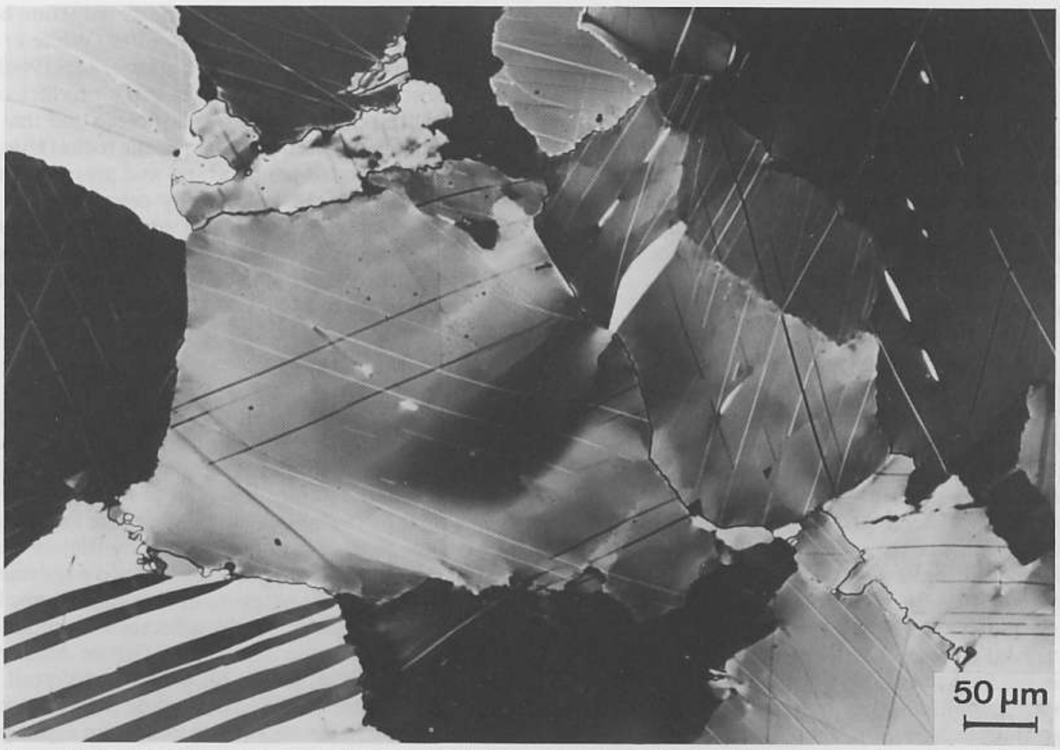


Fig. 3 Broad twin (t), causing inhomogeneous deformation in the form of a deformation band in a neighbouring grain which deforms by glide. Note bent twin lamellae indicating the strain associated with the deformation band. Carrara marble, experimentally deformed at 700°C, $10^{-3}s^{-1}$, 3 kb confining pressure and at 1150 bar differential stress by 13% shortening. Compression vertical.

dence is known as the Hall-Petch law in materials science (Nicolas and Poirier, 1976). The hardening effect of a small grain size is caused by the fact that the shear strain, as produced by the conservative motion of dislocations or by twinning within one grain, cannot simply be accommodated by the neighbouring grains which have different crystallographic orientations. Figure 3 illustrates this for the case of twinning in calcite. Olsson (1974) showed the Hall-Petch relationship to hold within a temperature range of 20–300°C in calcite rocks.

As a consequence of intracrystalline slip a crystallographic preferred orientation will develop (see section V).

Steady state is rarely achieved within this regime and in cases of work hardening many experimentalists formulate flow laws referring to an arbitrary level of strain (usually 10%).

### C. Power Law Creep

In many materials one observes a transition from an exponential stress dependence into power law creep (equation 3) with increasing temperature and decreasing stress. At the same time the apparent activation energies come to lie near the activation energies for diffusion. Microstructurally, one observes the formation of cells and subgrains on the TEM-scale and of optically visible subgrains under the optical microscope (Fig. 4). In a transient region from low temperature plasticity into power law creep core-mantle microstructures may be observed (Fig. 5), suggesting that subgrain formation first starts near the grain boundaries where strain compatibility reasons force the dislocations to rearrange into subgrain walls.

As in the domain of low temperature plasticity, dislocation glide is still the major strain producing mechanism and hence a crystallographic preferred orientation will develop. However, the arrangement of dislocations into subgrain walls is the rate controlling step. Thus, the strain rate at any given stress level is controlled by the velocity at which dislocations rearrange. They either have to climb or cross slip in order to leave the glide planes (Poirier, 1976). There is a great number of microdynamical models for power law creep (Poirier, 1976) and most of them predict an activation energy near that of lattice self diffusion, which in the specific case of dislocation climb creep (Weertmann, 1968) controls the climb velocity. The power $n$ in the power law for creep (equation 3) is predicted to be in the range from 3 to 5.

Dynamic recrystallization often accompanies power law creep and, together with subgrain formation and other manifestations of a recovery process, helps to keep the dislocation density sufficiently low to avoid strain hardening. In section IV specific mechanisms of recrystallization will be discussed in more detail.

The notion that dislocation density and the sizes of TEM-subgrains, optical subgrains and recrystallized grains should be in equilibrium at a given differential stress is only valid and applicable to paleostress determinations, provided that the rock deformed in the regime of power law creep (see discussion in chapter D).

The rheology of materials in the power law creep region is largely independent of the starting grain size.

A large number of experimentally determined flow laws have been obtained on rocks deformed within the field of power law creep (Carter, 1976; Tullis, 1979).

### D. Grain Size Sensitive Creep

At even higher temperatures and lower stresses, and/or for fine-grained materials there exists a number of mechanisms which are grain size sensitive in the sense that fine-grained materials are less flow resistant and where:

$$e \propto d^{-b} \quad (4)$$

where $d$ is the grain size and $b$ an exponent in the range 2–3. The deformation of the polycrystalline aggregate takes place by either diffusional mass transfer (diffusional flow and


Fig. 4 Optically visible subgrains in Carrara marble, experimentally deformed at 1000°C, $10^{-5}s^{-1}$, 3 kb confining pressure and at 132 bar differential stress by 32% shortening. Compression vertical.

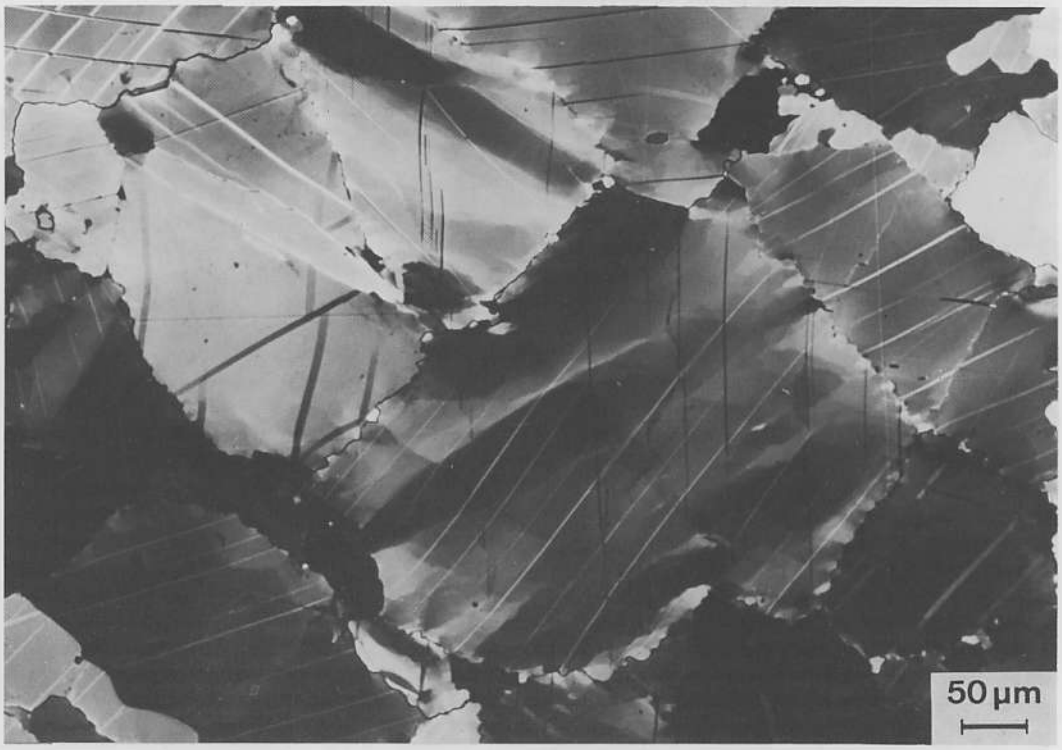


Fig. 5 "Core-mantle" structure in Carrara marble experimentally deformed at 700°C, $10^{-5}s^{-1}$, 3 kb confining pressure and at 685 bar differential stress by 12% shortening, compression vertical. Note that equiaxed subgrains are confined to the grain boundary regions, whereas deformation bands are characteristic for the grain interior.

pressure solution) or by sliding along grain boundaries of essentially rigid crystallites (superplasticity).

*Diffusional flow* in the solid state via migration of point defects along a stress gradient is known as Nabarro-Herring or Coble creep, depending on whether diffusion occurs through the lattice in the grain interior or near grain boundaries. For strain compatibility reasons, sliding at grain boundaries has to occur but the grain boundary shear stresses are so low that diffusion remains the rate controlling step during deformation (Beeré, 1978). The strain rate can be calculated from first principles by considering the stress dependence of the equilibrium density of point defects (for a simple derivation see Poirier, 1976). It has the form:

$$\dot{e} = C\, D_{eff}\sigma\Omega/kTd^2 \qquad (5)$$

where $C$ is a geometrical constant, $D_{eff}$ is the effective diffusion coefficient, $\Omega$ is the atomic volume and $d$ is the grain size. The effective diffusion coefficient is made up of two components: the lattice diffusion component dominating in Nabarro-Herring creep and the grain boundary diffusion component dominating in the Coble creep field. In the latter case the effective diffusion coefficient is inversely proportional to the grain size and thus the exponent b in equation 4 is equal to 3.

There is as yet no experimental evidence for solid state diffusional flow in rock materials. Diffusional flow is likely to occur at very low stresses and high temperatures only.

*Pressure solution*, involves diffusional mass transport in an aqueous environment via solution and redeposition of material (Fig. 6). It is a widespread mode of deformation in low grade rocks (Durney, 1972) but hard to observe under laboratory conditions because it is expected to dominate at low temperatures and stresses and at very slow strain rates only (Rutter, 1976). Rutter (1976) derived a constitutive equation for pressure solution on the domain of individual grains (Fig. 6) whose formalism is analogous to the equation for Coble creep: instead of a gradient in the equilibrium concentration of vacancies along the grain boundary there is a difference in solubility in the fluid films at the grain boundaries. The rate of deformation also depends on the grain boundary diffusivity in the presence of a fluid film.

The situation becomes more complex however if the solution transfer occurs over much larger distances as, for example, from a stylolite to a calcite vein (Durney and Ramsay, 1973). Such a situation can no longer be described in terms of a microdynamical model.

Another kind of grain size sensitive creep, likely to operate at low stresses and small grain sizes, is grain boundary sliding leading to *superplastic flow*. In this case grain boundary sliding acts as the prime strain producing mechanism and it is not just a consequence of strain compatibility problems as is the case during diffusional creep. Also the grains are now free to rotate and to switch neighbours after high amounts of strain (Edington *et al.*, 1976). Microdynamical models for superplastic flow usually assume that the strain rate is not controlled by the viscous resistance to gliding at grain boundaries but by the slowest event during sliding, namely the minor changes in shape the grains have to undergo in order to slide past each other. Ball and Hutchinson (1969) proposed that dislocations pile up at unfavourably oriented grain boundaries and that these dislocations escape by climbing into the grain boundaries. An alternative model by Ashby and Verrall (1973) proposes local diffusional mass transfer along grain boundaries.

In contrast to diffusional creep and pressure solution, a non-linear strain rate vs. stress relationship is observed, but the value of the exponent $n$ in equation 3 is always smaller than 3. The grain size exponent $b$ in equation 4 is usually found to lie between 2 and 3.

There is some ambiguity about the term superplasticity. In a wider sense, the notion of superplastic flow is a phenomenological one and just implies extreme ductility during an extension experiment, a common mode of testing metals. Ductility is a measure of resistance to necking in a tensile test and not directly related to a specific mechanism. In geology, the term superplastic in this wide sense can be used for any rock which is highly strained, such as any mylonite.


Fig. 6 Pressure solution on the scale of individual grains in a crinoidal limestone. Solution took place along horizontally oriented stylolites, the white redeposition areas grow in crystallographic continuity over the dark grey impure original single crystals of calcite.

High ductility and resistance to necking are however related to the deformation mechanism indirectly through the value of the parameter $n$ in equation 3. If $n = 1$ necks do not propagate (Gittus, 1978) and therefore materials deforming by diffusional creep can be referred to as being superplastic too in this wide sense.

In a more restricted sense however superplasticity implies that:

(i) grain boundary sliding is the major strain-producing mechanism,
(ii) that the microstructure remains stable, i.e. that the grains remain equiaxed even after large amounts of strain and
(iii) that the stress sensitivity of strain rate in terms of the parameter in equation 3 is between 1 and 3.

All these criteria do not apply in the case of diffusional creep, so here the term superplasticity will be used in this narrow sense.

Superplastic flow in rock materials has only recently been reported (Bouiller and Gueguen, 1975; Schmid *et al.*, 1977). It is difficult however to find direct evidence for grain boundary sliding in naturally deformed rocks and a stable microstructure can also be explained by dynamic recrystallization during power law creep. It is only the absence of a strong crystallographic preferred orientation which can indicate that grain boundary sliding may be the dominant strain producing mechanism.

## IV. Paleostress Estimates

### A. Estimates Based on the Extrapolation of Flow Laws

Ideally, the magnitude of differential stress can be estimated by extrapolation of laboratory determined flow laws into geological conditions on the basis of a deformation mechanism map, provided that there are independent estimates of strain rate and temperature. These extrapolations heavily rely on the accuracy of the deformation mechanism maps used, and thus also on the reliability of the theoretically calculated flow laws for regimes outside the range of experimental conditions accessible to the experimentalist.

Most of the experimentally determined flow laws apply to the mechanisms of low temperature plasticity and power law creep (for reviews see Carter, 1976; Tullis, 1979). Stresses operating during brittle fracture and cataclastic flow can be estimated through the well known Mohr-Coulomb criterion. Flow laws for grain size sensitive creep are available only for superplastically deformed calcite and olivine (Schmid *et al.*, 1977; Twiss, 1977 on the basis of data by Post, 1973, 1977).

Figure 7 is a graphical synopsis of some of the laboratory derived flow laws on various monomineralic rocks in the coordinates of a deformation mechanism map (compare Fig. 7). Possible transitions into cataclastic flow at high stresses (depending on confining pressure) and into grain size sensitive creep laws at low stresses are not considered in this figure because of the lack of experimental data (except for fine-grained limestone, deforming superplastically at low stresses). The curves are drawn for geologically realistic strain rates by simple extrapolations of empirical flow laws and they exhibit a more or less drastic drop in strength at vastly different temperatures. The relative strength of these materials corresponds nicely to the relative competence of these rocks in the field.

The slope at constant strain rate, as derived from a power law relationship (equation 3) is given by:

$$d \log \sigma / dT = -\frac{H}{2{\cdot}3\ RnT^2} \qquad (6)$$

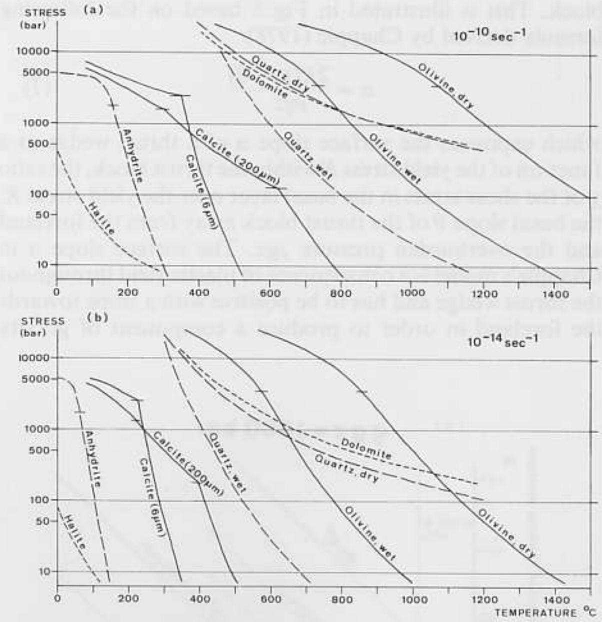


Fig. 7 Synoptic diagrams for constant strain rates of $10^{-10}s^{-1}$ (a) and $10^{-14}s^{-1}$ (b) illustrating the relative strength of different rock types as a function of temperature. The constant strain rate contours are based on experimentally determined flow laws for polycrystalline aggregates of halite (Heard, 1972), anhydrite (Müller and Briegel, 1980), fine-grained limestone (Schmid *et al.*, 1977), coarse-grained marble (Schmid *et al.*, 1980), wet and dry quartz (Parrish *et al.*, 1976), dolomite (Heard, 1976) and dunite (Post, 1977).

and depends not only on the apparent activation energy for creep but also on the value of the stress exponent $n$.

It is readily seen that accurate stress estimates are difficult because temperature estimates are usually not too precise. Also there are dependencies on water content in the case of the silicates and the limestone data emphasize the importance of grain size (note the reversal in relative strength of the two calcite rocks from the high stress area into the low stress area). On top of these difficulties come some of the problems discussed in the previous chapters.

Figure 7 however illustrates the vast differences in flow stress to be expected between different materials under conditions of constant strain rate. In reality, these differences are relaxed by inhomogeneous deformation and salt, anhydrite and limestone in particular are good decollement horizons at moderate temperatures, where dolomite and the silicates remain essentially brittle. Müller and Hsü (1980) showed by numerical modelling that the decollement of the Swiss Jura mountains including the Swiss molasse basin is compatible with the experimentally determined flow laws for anhydrite (Müller *et al.*, 1981), a major constituent within the Triassic evaporites.

At somewhat more elevated temperatures calcite may become an important decollement horizon provided that it deforms by superplastic flow. Based on the flow law for superplastically deformed limestone, the flow stress at the base of the Glarus overthrust and within a thin calc-mylonite layer (Schmid, 1975) can be estimated to be lower than 100 bar at the estimated temperatures and strain rates. New microfabric work on this mylonite horizon produced evidence that grain boundary sliding is the operative deformation mechanism (Schmid *et al.*, 1981).

The relative strength of decollement horizons and thrust blocks also has a major influence on the questions of gravity spreading versus active tectonic push at the rear of a thrust block. This is illustrated in Fig. 8 based on the following formula derived by Chapple (1978):

$$\alpha = \frac{2K(\frac{\chi}{2} - \theta)}{\rho g z} \quad (7)$$

which expresses the surface slope $\alpha$ of a thrust wedge as a function of the yield stress $K$ within the thrust block, the ratio $\chi$ of the shear stress in the basal layer over the yield stress $K$, the basal slope $\theta$ of the thrust block away from the foreland and the overburden pressure $\rho gz$. The surface slope $\alpha$ in Chapple's model is a consequence of plastic yield throughout the thrust wedge and has to be positive with a slope towards the foreland in order to produce a component of gravity

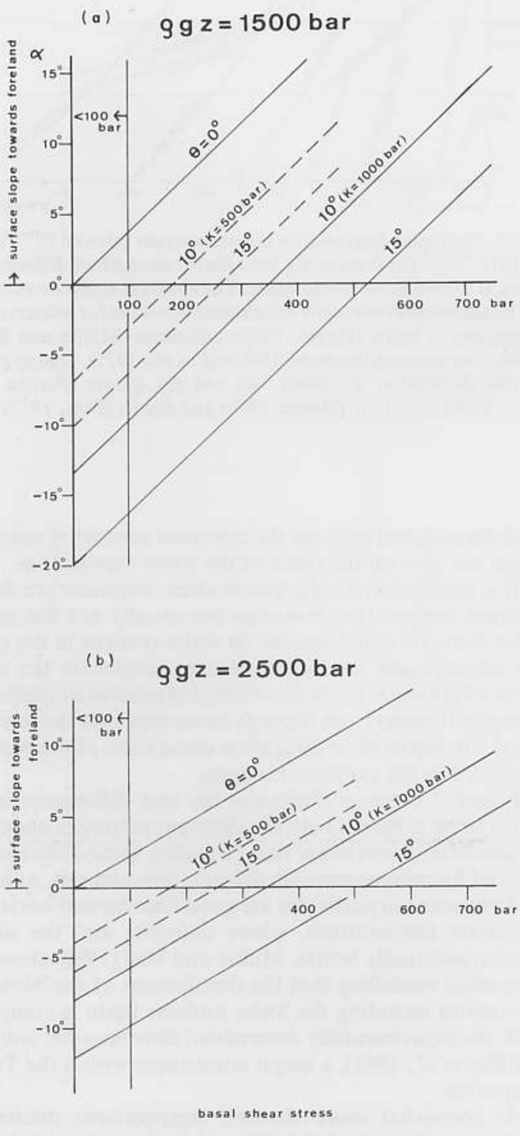


Fig. 8 Graphical representation of equation 6 discussed in the text (Chapple, 1978, equation 36). This graph illustrates the dependence of the surface slope $\alpha$ on the absolute value of the basal shear stress in decollement or mylonite horizon. Two sets of contours are given for a 0°, 10° and 15° slope $\theta$ of the basal decollement horizon away from the foreland: the solid and broken lines assume a yield stress K of 1000 bar and 500 bar respectively. The top figure (a) refers to a thickness of the overthrust block of 6 km, the bottom figure (b) assumes 10 km overburden. Notice that positive surface slopes, and consequently a component of gravity spreading are only obtained for relatively strong decollement horizons (far in excess of 100 bars considered to be the maximum shear strength of a mylonite such as the Lochseiten mylonite at the Glarus overthrust).

spreading in the driving force. Figure 8 illustrates that for basal shear stresses of less than 100 bars, expected for decollement horizons such as evaporites and limestones, the resulting surface slope $\tau$ is negative and thus gravity spreading must be ruled out in such cases.

Because negative surface slopes away from the foreland are geologically unrealistic, Chapple's assumption of pervasive yield within thrust wedges has to be relaxed if the basal shear stress is very much lower than the yield stress within the thrust wedge. It can be shown in the case of the Helvetic nappes of eastern Switzerland that internal deformation within the Helvetic thrust block predates the final phase of thrusting (Schmid, 1975; Milnes and Pfiffner, 1977). The gravity spreading concept and Chapple's model however certainly apply for cases where there is a more homogeneous stress distribution in basal decollement horizon and thrust wedge.

## B. Paleostress Determinations Based on Microstructural Information

### 1. *Stress directions*

The classic methods for the derivation of stress directions based on twinning in calcite and dolomite (Turner and Weiss, 1963) have been further developed by Spang (1972) and they have been applied for mapping of principal stress directions in cross-sections through the Rocky Mountains (Spang and Brown, 1981). These methods rely on the fact that twinning in calcite and dolomite can only be operated in a unique shear sense relative to the crystallography, contrary to slip systems which generally have no prescribed sense of shear. This method however only works for moderately strained rocks where twinning did not go to near-completion.

Other, similar, methods which can only be applied in the brittle field rely on fracture patterns, slickensided faults and fault plane solutions.

### 2. *Stress magnitude*

There is a number of methods to determine the paleostress from microstructural data and these methods have received a lot of attention during the last few years. The dislocation density of free dislocations, the size of subgrains and the size of dynamically recrystallized grains have been used to infer paleostress. The equations relating these microstructural parameters to differential stress are partly based on theoretical considerations and partly on the empirical laboratory calibrations which are available for a number of minerals (for reviews see Nicolas and Poirier, 1976; Mercier *et al.*, 1977; Twiss, 1977; White, 1979).

There are a number of difficulties associated with these methods:

1. All of these methods assume a steady state microstructure which developed under dynamical conditions during power law creep. They are not valid for all the other deformation regimes and in situations of strain hardening or strain softening their use becomes, at the very least, problematic.
2. The microstructural imprint of the main phase of steady state deformation in which the geologist is interested may be overprinted by the later geological history. Dislocation density in particular is very susceptible to late overprints associated with small amounts of strain. The most stable paleostress indicator is probably the recrystallized grain size and the discussion will focus on some of the problems associated with this particular method.

The recrystallized grain size $d$ is related to differential stress through:

$$\sigma/\Gamma = K(d/b)^{-p} \qquad (8)$$

where $\Gamma$ (an elastic modulus related to the shear modulus and Poissons ratio) and $b$ (the Burgers vector) are used to normalize stress and grain size into dimensionless quantities and $K$ and $p$ are constants (see Twiss, 1977).

Figure 9 summarizes the data available for various minerals. The scatter in Fig. 9a becomes somewhat reduced by normalizing stress and grain size according to the equation given above (Fig. 9b); the slope $p$ however still varies between values of 0·67 and 1·43 (for the same mineral, olivine). Using theoretical arguments, Twiss (1977) predicted slopes of 1·0 and 0·7 for subgrains and recrystallized grains respectively.

The large scatter suggests that these calibrations should be applied to geological situations with caution and that paleostress determinations are only order-of-magnitude estimates. The scatter may have several reasons:

1. There are problems with the technical determination of grain size (for a discussion of the methods, see Etheridge and Wilkie, 1981).
2. Other factors such as temperature, water content, impurities and second phase minerals may also have an influence on the final grain size. Static thermal treatment after the experiment may lead to grain growth (annealing recrystallizaton). Water demonstrably has an effect on the grain size (Fig. 9), whilst impurities and second phase minerals may pin the grain boundaries.
3. There are several mechanisms of recrystallization which may lead to different grain sizes. Apart from annealing recrystallization, not related to stress, there are the following categories of mechanisms during dynamic (= syntectonic) recrystallization: the *rotation* mechanism involves the relative rotation of subgrains as a consequence of adding more dislocations on the same sign into a subgrain boundary (Hobbs, 1969; Nicolas and Poirier, 1976). This mechanism is sometimes referred to as *"in situ"* recrystallization and it is a mere extension of recovery processes (Sellars, 1977). The *migration* mechanism keeps the dislocation density low by the movement or migration of high angle boundaries from grains with a low dislocation density into neighbouring grains with a higher density (Poirier and Guillopé, 1979). Finally Mercier *et al.* (1977) invoked models of *nucleation and growth* of new grains from preformed "nuclei" such as subgrains, deformation bands and grain boundary bulges.

Guillopé and Poirier (1979) have demonstrated that, in the case of halite, the grain size for grains recrystallized by migration is larger than the grain size produced by the rotation mechanism (Fig. 9). In this case the two mechanisms operate simultaneously above a critical temperature, an observation made for the case of calcite as well (Schmid *et al.*, 1980). For quartz and olivine however the mechanisms of recrystallization are not known or specified in the literature. While Hobbs (1969) and Poirier and Nicolas (1975) infer rotation mechanisms for quartz and olivine respectively, Mercier *et al.* (1977) and Ross *et al.* (1980) prefer the nucleation and growth model. Kirby and Green (1980), in a study of dunite xenoliths, observe recrystallization by a migration mechanism.

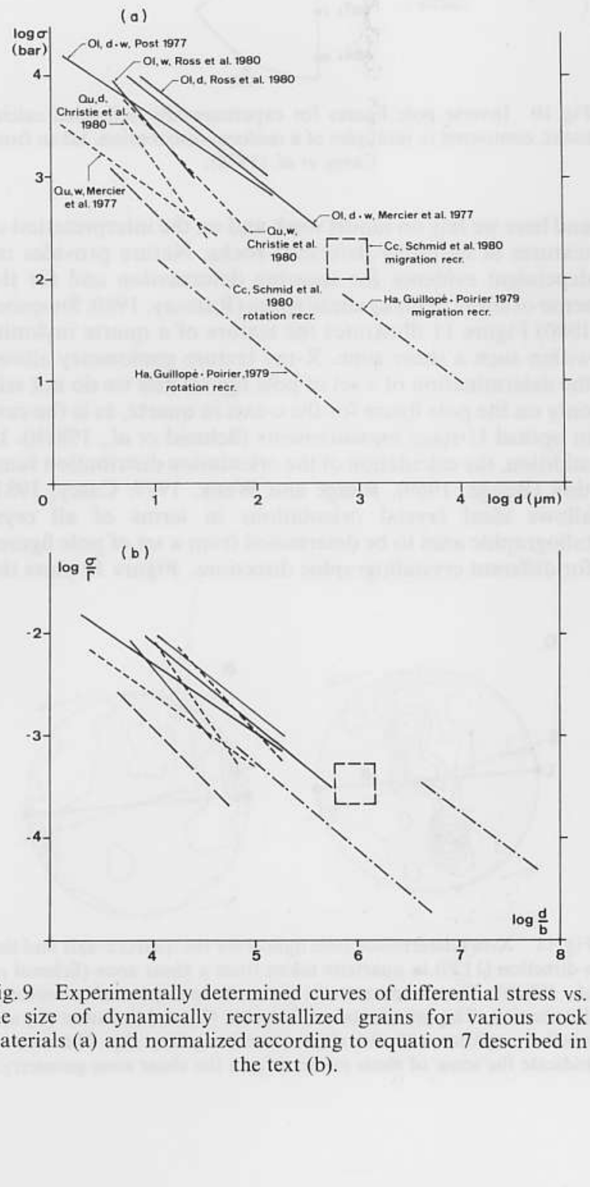


Fig. 9 Experimentally determined curves of differential stress vs. the size of dynamically recrystallized grains for various rock materials (a) and normalized according to equation 7 described in the text (b).

This discussion on recrystallization mechanisms indicates that a better understanding of the mechanisms of recrystallization is needed for more accurate stress determinations. In the case of quartz, there are some data available now for naturally deformed rocks (see review by Etheridge and Wilkie, 1981). The magnitudes of differential stress all vary between a few hundreds of bars up to the order of 1 kbar. These estimates are probably relatively reliable because no great extrapolations from laboratory stresses down to the estimated geological stresses are involved. In olivine, the situation is different in that the stress estimates for the upper mantle (below 100 bars, Ave Lallemant *et al.*, 1980) involve an extrapolation of about an order of magnitude in differential stress (most experiments were performed at stresses above 1 kb in solid medium equipment).

In spite of all these difficulties, the paleostress determinations have given us direct information on the order of magnitude of differential stresses active during power law creep in naturally deformed rocks. Even lower stresses should not be excluded, however, for the case of grain size sensitive creep.

## V. Crystallographic Preferred Orientation (Texture)

This topic offers a particularly good example of the progress made over the past few years through a combined effort from both the experimental approach and from attempts to simulate the development of crystallographic preferred orientation (which will be referred to as texture here, following the materials science terminology) by using computer based numerical models. There is a vast amount of texture data in the geological literature, but in many cases interpretations of the pole figures have remained highly speculative and sometimes nebulous.

The work of Lister and co-authors (Lister *et al.*, 1978; Lister and Paterson, 1979; Lister and Hobbs, 1980) in particular made it very clear that texture development is governed by three main factors:

1. *The particular set of glide systems active during deformation.* This produces characteristic patterns from which we can learn about the stress, strain rate and temperature conditions during deformation (Lister and Paterson, 1979). Experimental work on single crystals provides important input parameters for these numerical models in providing information on the relative magnitudes of the critical resolved shear stresses needed to operate particular glide systems as a function of the environmental parameters.
2. *Finite strain.* With the same set of active glide systems the type of finite strain (flattening, constriction, plane strain etc.) produces different pole figure patterns (Lister and Hobbs, 1980). In the case of texture development through glide-induced lattice rotations, as modelled by Lister and co-authors, it is difficult to estimate the magnitude of strain. For an alternative mechanism, such as the passive rotation of sheet silicates in a ductile matrix, attempts have been made to relate the strength of the texture to the strain magnitude (March, 1932).
3. *The strain path or the kinematic framework.* The influence of these on the final texture pattern has been studied by Lister and Hobbs (1980) and Etchecopar (1977). Starting with a random texture and excluding complex multiphase strain histories, an asymmetry of the pole figures in respect to the macroscopic fabric axes (foliation, lineation) is indicative for a non-coaxial strain path with a large component of simple shear and the sense of the asymmetry reflects the sense of shear.

   It is still not clear how much and in exactly which way intracrystalline slip occurring in low temperature plasticity and power law creep determines the lattice rotations of individual grains. Many rocks with a strong texture are dynamically recrystallized and dynamic recrystallization was not considered by the model work of Etchecopar (1977) and Lister *et al.* (1978).

Figure 10, taken from Casey *et al.* 1978, is a good example for how the deformation mechanisms and the set of active glide systems influence the texture in the case of calcite. The type 1 textures (Fig. 11) are indicative of twinning, known to be the easiest glide system at low temperatures. The type 2 textures occur in the absence of twinning and Lister (1978) simulated this texture remarkably well by activating slip mainly on the rhombs r and f. The type 3 textures are comparatively weak and the transition from type 2 into type 3 exactly coincides with the change in deformation mechanism form power law creep into superplastic flow (Schmid *et al.*, 1977; Casey *et al.*, 1978). The fact that a weak texture does develop indicates that some intracrystalline slip takes place during grain boundary sliding.

Usually the laboratory experiments produce uniaxially deformed specimens and, as a consequence of this, the pole figures exhibit rotational symmetry around the compression axis (this is the reason for using inverse pole figures for details; see Bunge, 1969). The experimental work of Kern (1971) is the only example of a more complex type of coaxial strain and he experimentally demonstrated how the type of strain influences the texture.

Experiments in simple shear are very difficult to perform

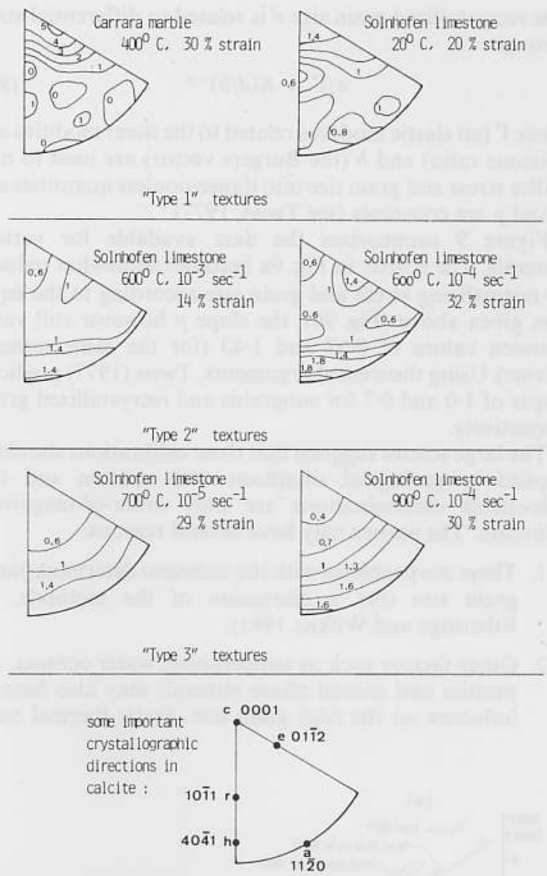


Fig. 10 Inverse pole figures for experimentally deformed calcite rocks, contoured in multiples of a uniform distribution, taken from Casey *et al.* (1978).

and here we rely on model work and on the interpretation of textures in naturally deformed rocks. Nature provides independent evidence for shearing deformation and for the sense of shear in many shear zones (Ramsay, 1980; Simpson, 1980).Figure 11 illustrates the texture of a quartz mylonite within such a shear zone. X-ray texture goniometry allows the determination of a set of pole figures and we do not rely only on the pole figure for the c-axis in quartz, as is the case in optical U-stage measurements (Schmid *et al.*, 1981b). In addition, the calculation of the orientation distribution function (Bunge, 1969), Bunge and Wenk. 1977; Casey, 1981) allows ideal crystal orientations in terms of all crystallographic axes to be determined from a set of pole figures for different crystallographic directions. Figure 12 plots the

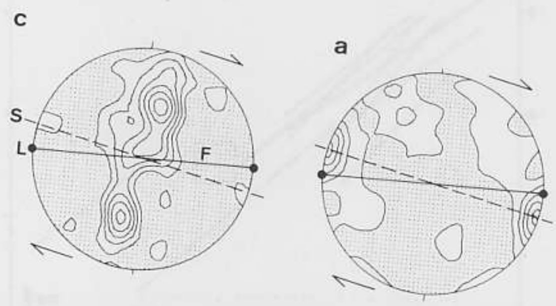


Fig. 11 X-ray determined pole figures for the quartz c-axis and the a-direction (1120) in quartzite taken from a shear zone (Schmid *et al.*, 1981b). The countours are given in multiples of a uniform distribution. The orientation of foliation (F) and lineation (L) are labelled together with the shear zone boundary (S). The arrows indicate the sense of shear inferred from the shear zone geometry.

most likely orientation of a quartz grain in case of the specimen presented in Fig. 11. The a-direction (normal to the second order prism in quartz), an important glide direction, is aligned with the inferred shear direction within the shear zone. In addition, the position of the c-axis suggests that the positive rhombs prefer to be aligned with the shear zone boundary and this is confirmed in Fig. 12. This is a stable orientation for easy glide on the rhomb planes and in the following chapter the rheological consequences of such a stable end-orientation will be discussed.

Figure 13 illustrates that this same specimen dynamically recrystallized, probably by a rotation mechanism. Dynamic recrystallization did not destroy the texture, which can still be readily interpreted in terms of intracrystalline slip. There is thus no need to invoke separate models of texture development for dynamically recrystallized grains, such as the Kamb model (see discussion in Nicolas and Poirier, 1976).

An immediate application of such asymmetries lies in the determination of shear sense, not known in many geological settings, and in kinematic interpretation of lineations in terms of a- and b-lineations following Sanders terminology. In our case, the lineation is at a small angle to the shear direction and therefore represents a stretching lineation subparallel to the relative displacement of the shear zone boundaries (a-lineation). There are now numerous examples of the determination of shear sense using this principle (Eisbacher, 1970; Boucher, 1978; Burg and Laurent, 1978; Bouchez and Pecher, 1981). Systematic regional studies on the significance of lineations for inferring the direction of relative displacement of nappes or during internal deformation of gneissic bodies will certainly be of major geotectonic importance in the future.

## VI. Strain Softening Mechanisms

Localized deformation in shear zones is an important mode of deformation in basement rocks (Ramsay, 1980) and ductile flow in mylonite layers accounts for large nappe translations. The formation of shear zones and mylonite horizons is a consequence of local shear instabilities. There is a variety of possible mechanisms which can lead to strain softening (see reviews by Poirier, 1980 and White *et al.*, 1980) and hence to shear instabilities. Although shear heating (Brun and Cobbold, 1980; Fleitout and Froidevaux, 1980) probably is the most popular softening mechanism, we will only discuss two other possible mechanisms, because they relate closely to the topics discussed so far:

(1) Geometrical softening caused by the rotation of easy glide systems into orientations of high resolved shear stresses during texture formation and

(2) softening as a consequence of a change in deformation mechanism from power law creep into grain size sensitive

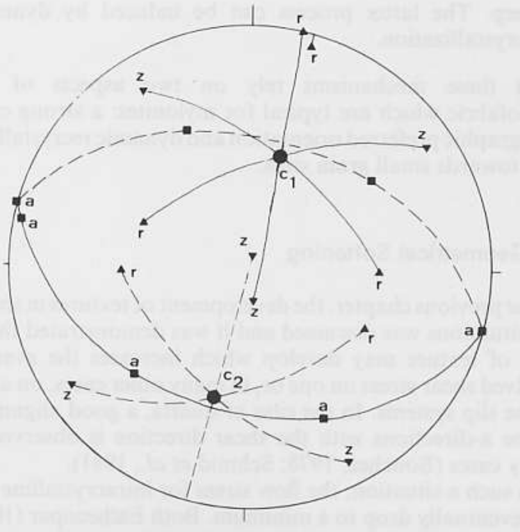


Fig. 12 Favoured crystal orientation for the specimen presented in Fig. 11. The c-axis position labelled $c_1$ and $c_2$ correspond to the positions of the c-axis maxima in Fig. 11, the positions of the poles to (11$\bar{2}$0) are labelled a (second order prisms), the positions of the poles to (10$\bar{1}$1) and (01$\bar{1}$1) are labelled r and z (positive and negative rhombs respectively).

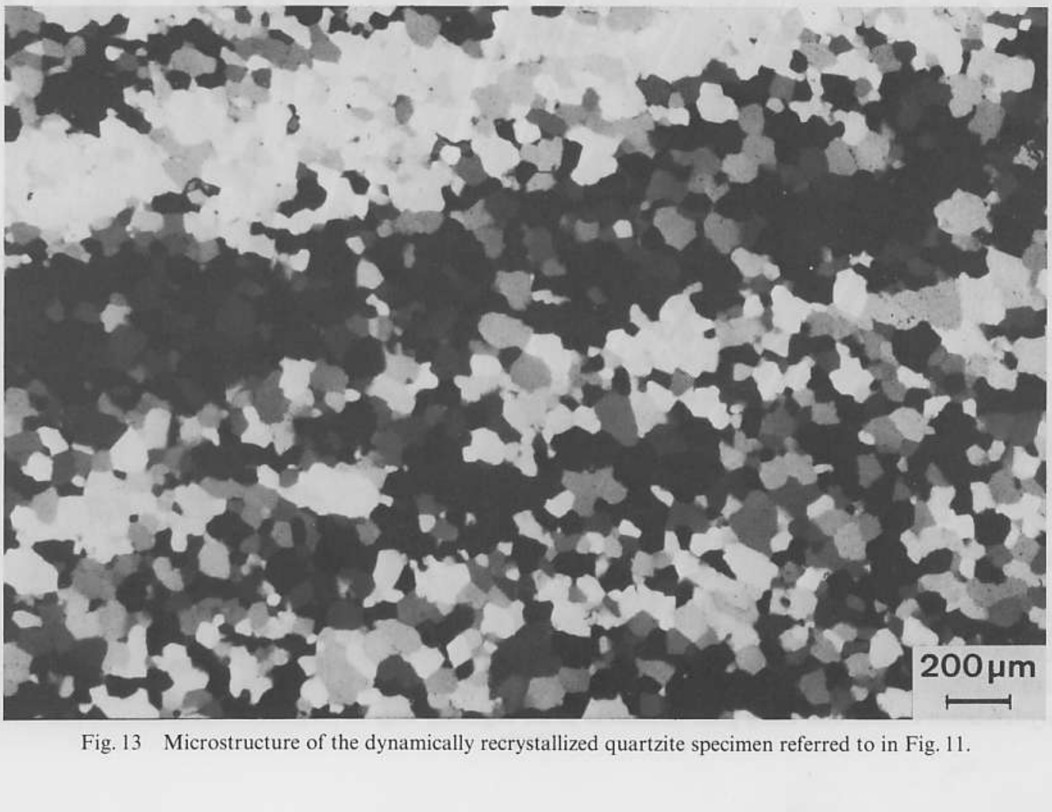


Fig. 13 Microstructure of the dynamically recrystallized quartzite specimen referred to in Fig. 11.

creep. The latter process can be induced by dynamic recrystallization.

Both these mechanisms rely on two aspects of the microfabric which are typical for mylonites: a strong crystallographic preferred orientation and dynamic recrystallization towards small grain sizes.

## A. Geometrical Softening

In the previous chapter, the development of textures in shearing situations was discussed and it was demonstrated that a type of texture may develop which increases the average resolved shear stress on one or, in many other cases, on a few of the slip systems. In the case of quartz, a good alignment of the a-directions with the shear direction is observed in many cases (Bouchez, 1978; Schmid *et al.*, 1981).

In such a situation, the flow stress for intracrystalline slip will eventually drop to a minimum. Both Etchecopar (1977) and Lister and Hobbs (1980) simulated the development of such end-orientations in their models.

Experimental data by Burrows *et al.* (1979) suggests that the reorientation of the lattice may be assisted by dynamic recrystallization and many mylonites with a strong texture are dynamically recrystallized. The mechanism of grain boundary migration in particular offers a good empirical explanation for the enhancement of the rate of reorientation of the crystal lattice towards an end-orientation for easy glide. Those grains which are unsuitably oriented for easy glide will accumulate high levels of internal elastic strain energy through a high dislocation density and lattice distortions in the form of undulouse extinction, kink bands, deformation bands etc. Grains oriented for easy glide on the other hand have a lower dislocation density and because they deform in compatibility with the bulk aggregate they store less elastic strain energy. This promotes the consumption of unsuitably oriented grains and hence strengthens the texture.

## B. Softening by a Strain Induced Change in Deformation Mechanism

Dynamic recrystallization during power law creep effectively changes the grain size of the starting material as illustrated in Fig. 5 for experimentally deformed calcite. The same process of grain size reduction in the case of the calc-mylonite along the Glarus overthrust in the Helvetic nappes of Switzerland is illustrated in Figs 14, 15, 16. For Fig. 16 it is particularly obvious that the mechanism of dynamic recrystallization by subgrain rotation induces the change in grain size.

The new recrystallized grain size has been determined to be around 6–7 μm and according to the stress vs. grain size relationship of Fig. 9 this indicates paleostresses of around 700 bar during subgrain formation and recrystallization in power law creep. As the initial grain size is reduced, grain size sensitive creep may or may not take over depending on the size of the new grains and the position of the mechanism boundary between power law creep and grain size sensitive creep. This will now be discussed in some detail on the basis of Fig. 17, which shows a deformation regime map with grain size as a variable at constant temperatures. This graph was constructed for calcite aggregates by combining the constitutive equations for exponential and power law creep as observed in Carrara marble (Schmid *et al.*, 1980) with those for superplastic flow observed in Solnhofen limestone (Schmid *et al.*, 1977). Because superplastic flow is grain size dependent, the resulting deformation regime boundary is grain size dependent as well and separates a high stress — large grain size area of predominantly power law creep from a low stress — small grain size area of superplastic flow.

Superimposed on this deformation regime map is the curve of stress vs. the size of new grains recrystallizing by a rotation mechanism of dynamic recrystallization (see Fig. 9). Strictly speaking this curve should fall within the power law field because this recrystallization by subgrain rotation can only be brought about by power law creep and the notion of an "equilibrium grain size" is meaningless in the domain of


Fig. 14 Recrystallization concentrated along grain boundaries at the beginning stage of progressive mylonitization. Lochseiten mylonite, Glarus.

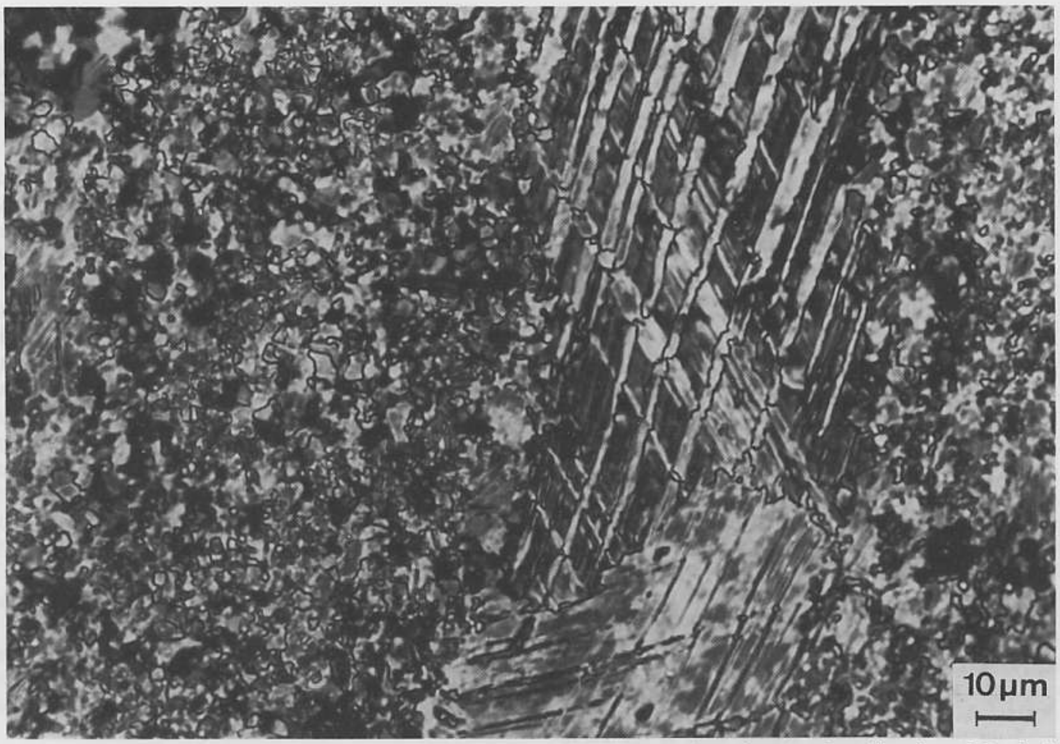


Fig. 15 Recrystallization to a new fine-grained aggregate in the matrix. Old grains (porphyroclasts) are heavily twinned. Lochseiten mylonite, Glarus.

superplastic flow (Etheridge and Wilkie, 1979). The stress vs. grain size curve however is superimposed on the deformation mechanism map solely for the purpose of demonstrating the following evolution with increasing strain:

A calcite aggregate deforms by a strain rate and under a stress indicated by the position of point A in Fig. 17. The position of this point A indicates that the material has a grain size which is larger than the size of the subgrains and recrystallized grains expected to form with increasing strain. The material deforming by dislocation creep at point A will eventually recrystallize to a grain size along a curve which comes to lie within the field of superplasticity. The paths to point B and C indicated in Fig. 17 indicate two extreme possibilities of what can hypothetically occur if the production of a new grain size by rotation recrystallization would

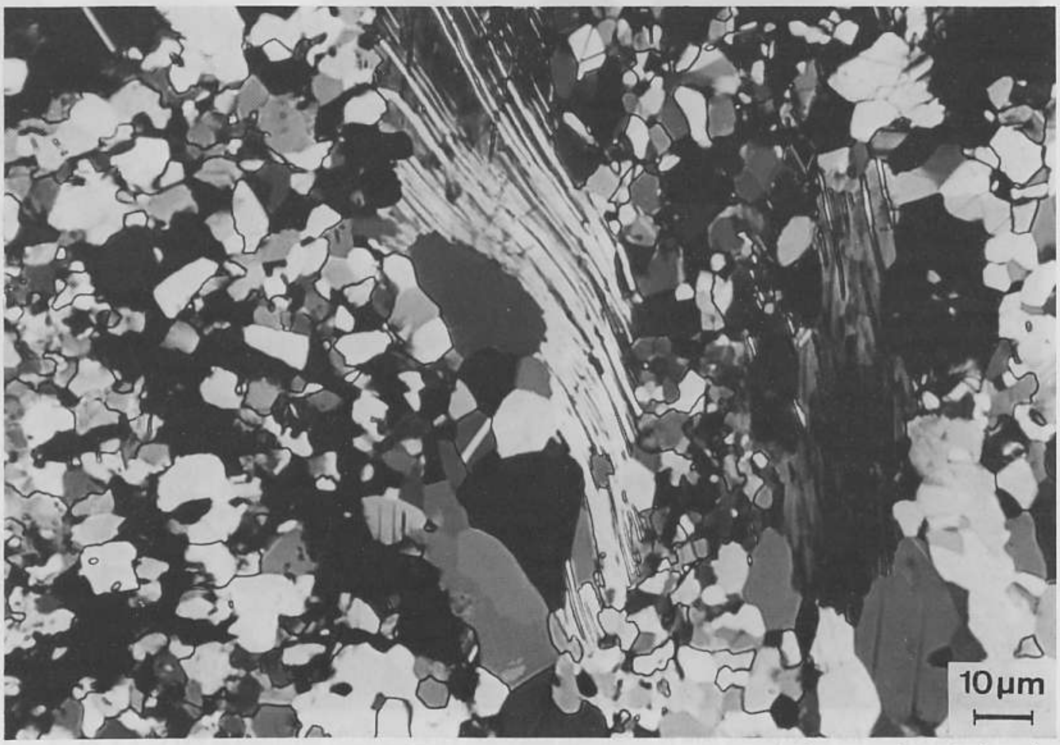


Fig. 16 Recrystallization went almost to completion. The new grains are free of optical strain features, the grain boundaries are well equilibrated (compare Fig. 18). Lochseiten mylonite, Glarus.

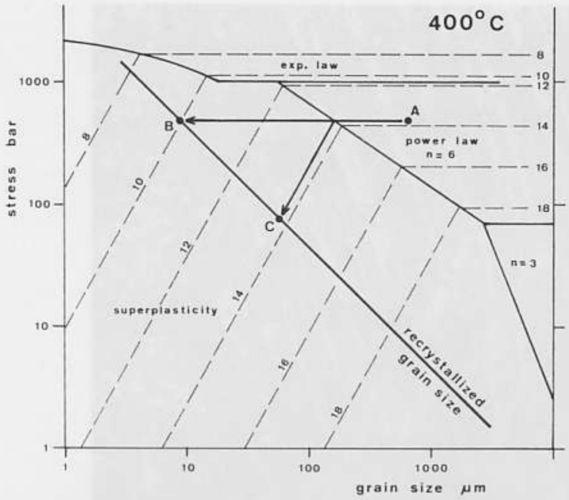


Fig. 17 Deformation regime map for calcite at a temperature of 400°C presented in differential stress vs. grain size coordinates. The strain rate contours are labelled with the negative exponent of the strain rate in $s^{-1}$. The map is based on experimentally determined flow laws of calcite. In the superplastic regime the equation for grain size sensitive creep of Solnhofen limestone was used (equation 2 in Schmid *et al.*, 1977). The flow laws for the exponential and power law regimes are taken from data on Carrara marble (Rutter, 1974; Schmid *et al.*, 1980, stress relaxation data).

Superimposed on this deformation regime map is the curve labelled recrystallized grain size taken from the calcite data presented in Fig. 9. For a discussion of this graph and the explanation of the points labelled A, B and C, see text.

be instantaneous. The case B illustrates that under boundary conditions of constant stress an acceleration of strain rate over several orders of magnitude will occur as a consequence of the change in grain size. The case C alternatively illustrates a stress drop under the extreme opposite boundary conditions of constant strain rate. This change in rheological behaviour can only occur if the position of the equilibrium grain size curve is inside the superplastic field. It is emphasized again that once the change in mechanism has occurred, the curve of recrystallized grain size vs. stress becomes meaningless.

However, it is obvious that instantaneous recrystallization is a very unreasonable assumption for what may occur in nature. As observed in the experiments on Carrara marble and also in many mylonitic rocks the evolution of an equiaxed fine-grained aggregate of recrystallized grains will lead to a bimodal grain size distribution. Some fabric domains will be fully recrystallized while the original grain size will be preserved in other domains. This may lead to a situation where both power law creep and superplasticity occur simultaneously in different fabric domains. Such a situation can no longer be described by a single point in the diagram of Fig. 17. Initially the fully recrystallized domains will be isolated and will make up a small volume fraction of the rock. Thus, flow will remain stable and can still be defined by the position of point A in Fig. 17. As the volume fraction of fully recrystallized material grows, the bulk strain rate of the rock will increase and/or the bulk stress will drop due to the contribution of the superplastically deforming domains to the overall deformation in the rock. The rheology of the bulk rock can then be thought to be given by the position of a point somewhere along the path between A and B or A and C.

In conclusion, dynamic recrystallization will induce a change in microstructure which in turn induces a change in deformation mechanism leading to work softening.

This conclusion apparently contradicts the fact that during experimental deformation of Carrara marble no work softening was observed as a consequence of dynamic recrystallization, even after more than 30% shortening (Schmid *et al.*, 1981). However, when a similar deformation regime map is constructed for the 900–1050°C temperature region (the temperatures at which recrystallization occurred in these experiments) one ends up with a different position of the

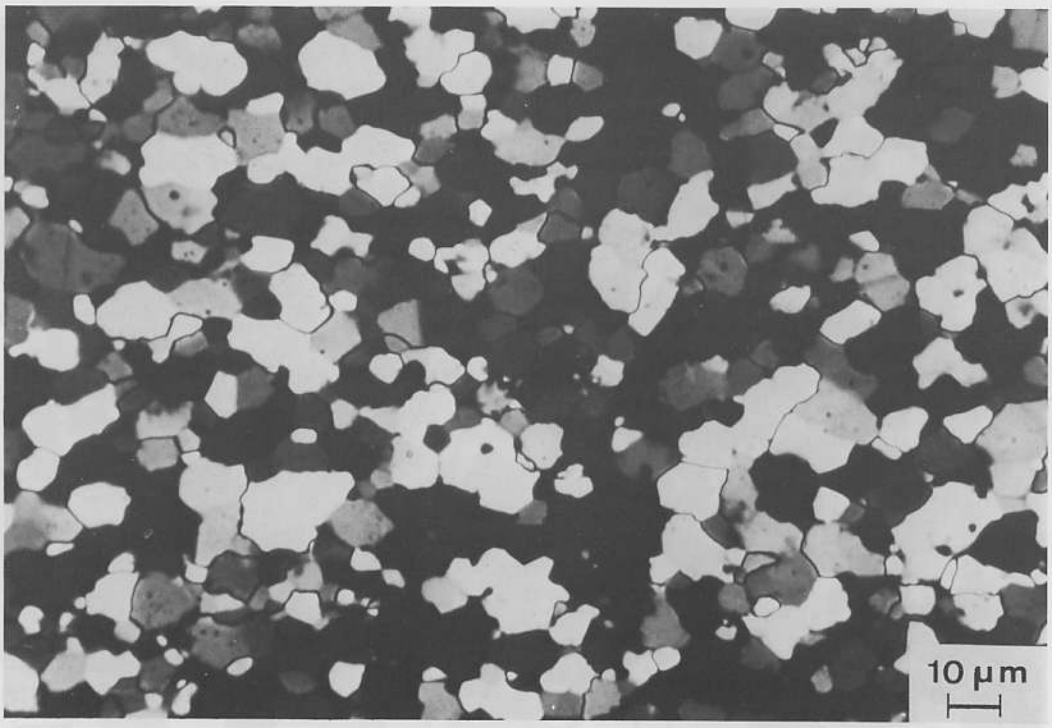


Fig. 18 Microstructure, typical for superplastic flow in Solnhofen limestone, experimentally deformed at 900°C, $7 \times 10^{-4} s^{-1}$, 3 kb confining pressure and at 280 bar differential stress by 36% shortening. Note the well equilibrated grain boundaries and the absence of grain flattening in spite of the large amount of strain.

mechanism boundary in stress vs. grain size coordinates due to the different activation energies for creep in dislocation creep and superplastic flow respectively. The mechanism boundary now almost coincides with the position of the equilibrium grain size curve or comes to lie inside the dislocation creep field. In other words, the new grain size produced by recrystallization does not fall inside the area of dominantly superplastic flow at the high temperatures and therefore no work softening is expected. The mechanism of work softening proposed here is thus expected to be important at relatively low temperatures.

In the case of the calc-mylonite mentioned earlier it is very likely that the stress estimate of 700 bars is only valid for the initial deformation within the power law creep field. The similarity between the final microstructure of this mylonite, after recrystallization is almost complete (Fig. 16), and the microstructure of superplastically deformed Solnhofen limestone (Fig. 18) is striking. The texture of totally recrystallized specimens of this mylonite is very weak (Schmid *et al.*, 1981a). This suggests that a change in mechanism into superplastic flow has occurred and thus the paleostress estimate of 700 bar is no more valid for the final phase of thrusting.

The same mechanism of work softening presented here may also apply for other rock types. Bouiller and Gueguen (1975) describe superplastic mylonites in peridotites and Twiss (1976) interpreted ductile show zones in the experiments of Post (1973) in terms of a mechanism change induced by dynamic recrystallization.

Above, work softening as a consequence of a change in deformation mechanism towards grain boundary sliding (superplasticity) was discussed. A similar weakening effect as a consequence of grain size reduction can of course be postulated for transitions into other grain size sensitive deformation mechanisms such as pressure solution or diffusional creep.

## Discussion

There is no doubt that the concept of plate tectonics leads to a better understanding of the process of mountain building in terms of unifying many aspects of geoscience into a coherent framework. The problem of identifying the driving forces in mountain building however, is still largely unresolved. The choice between alternative models such as the gravity spreading model versus active tectonic push on the scale of individual nappes can only rarely be made on the basis of geometrical considerations and it was demonstrated that knowledge about the relative rock strength may provide additional constraints. On a larger scale, the question after the driving forces of plates has to be answered and here again critical information on the rheology of lithosphere and asthenosphere can be provided by laboratory investigations.

The specific applications discussed showed that laboratory studies have already had a considerable impact on our understanding of deformation processes in geological environments via microfabric studies. If this dicussion helps to stimulate further work in terms of a combined effort from the field geological, modelling and experimental sides the main purpose of this contribution is met.

## References


Ashby, M.F. and Verrall, R.A. (1973). Diffusion-accommodated flow and superplasticity. *Acta Met.* **21,** 149–163.

Ashby, M.F. and Verrall, R.A. (1978). Micromechanisms of flow and fracture and their relevance to the rheology of the upper mantle. *Phil. Trans. R. Soc. Lond. A* **288,** 59–95.

Ave Lallement, H.G., Mercier, J.-C.C., Carter, N.L. and Ross, J.V. (1980). Rheology of the upper mantle: Inferences from peridotite xenoliths. *Tectonophysics* **70,** 85–113.

Ball, A. and Hutchinson, M.M. (1969). Superplasticity in the Aluminium-Zinc Eutectoid. *Metal Science Journal* **3,** 1–7.

Beeré, W. (1978). Stresses and deformation at grain boundaries. *Phil. Trans. R. Soc. Lond. A* **288,** 177–196.

Bouchez, J.L. (1978). Preferred orientation of quartz (a) axes in some tectonites. *Tectonophysics* **49,** T25–T30.

Bouchez, J.L. and Pecher, A. (1981), The Himalayan Main Central Thrust Pile and its quartz-rich tectonites in Central Nepal. *Tectonophysics* **78,** 23–50.

Bouiller, A.M. and Gueguen, Y. (1975). Origin of some mylonites by superplastic flow. *Contr. Min. Pet.* **50,** 93–104.

Brun, J.P. and Cobbold, P.R. (1980). Strain heating and thermal softening in continental shear zones: a review. *J. Struct. Geol.* **2,** 149–158.

Bunge, H.J. (1969). Mathematische Methoden der Texturanalyse. Akademie Verlag, Berlin, 330 pp.

Bunge, H.J. and Wenk, H.R. (1977). Three dimensional analysis of three quartzites (triginal crystal and triclinic specimen symmetry). *Tectonophysics* **40,** 357–385.

Burg, J.P. and Laurent, Ph. (1977). Strain analysis of a shear zone in a granodiorite. *Tectonophysics* **47,** 15–42.

Burrows, S.E., Humphreys, F.J. and White, S.H. (1979). Dynamic recrystallization and textural development in magnesium deformed in compression at elevated temperatures. 5th Int. Conf. on Strength of Metals and Alloys, Aachen, 607–615.

Carter, N.L. (1976). Steady state flow of rocks. *Rev. Geophys. Space Phys.* **14,** 301–360.

Carter, N.L., Christie, J.M. and Griggs, D.T. (1964). Experimental deformation and recrystallization of quartz. *J. Geol.* **72,** 687–733.

Casey, M. (1981). Numerical analysis of X-ray texture data: An implementation in Fortran allowing triclinic or axial specimen symmetries. *Tectonophysics* **78,** 51–54.

Casey, M., Rutter, E.H., Schmid, S.M., Siddans, A.W.B. and Whalley, J.S. (1978). Texture development in experimentally deformed calcite rocks. Proc. 5th Int. Conf. on Textures of Materials, Aachen, Springer Verlag, Berlin, p. 231–240.

Chapple, W.M. (1978). Mechanics of thin-skinned fold-and-thrust belts. *Geol. Soc. Am. Bull* **89,** 1189–1198.

Christie, J.M., Ord, A. and Koch, P.S. (1980). Relationship between recrystallized grain size and flow stress in experimentally deformed quartzite. *EOS* **61,** 377.

Durney, D.W. (1972). Solution transfer, an important geological deformation mechanism. *Nature, London* **235,** 315–317.

Durney, D.W. and Ramsay, J.G. (1973). Incremental strains measured by syntectonic growths. *In* "Gravity and Tectonics" (DeJong, K. and Scholten, R., eds). Wiley, New York, pp. 67–96.

Edington, J.W., Melton, K.N. and Cutler, C.P. (1976). Superplasticity. *Progr. Mater. Sci.* **1,** 61–158.

Eisbacher, G.H. (1970). Deformation mechanics of mylonite rocks and fractured granulites in Cobequid Mountains, Nova Scotia, Canada. *Geol. Soc. Am. Bull.* **81,** 2009–2020.

Etchecopar, A. (1977). A plane kinematic model of progressive deformation in a polycrystalline aggregate. *Tectonophysics* **39,** 1–3, 121–139.

Etheridge, M.A. and Wilkie, J.C. (1979). Grainsize reduction, grain boundary sliding and the flow strength of mylonites. *Tectonophysics* **58,** 159–178.

Etheridge, M.A. and Wilkie, J.C. (1981). An assessment of dynamically recrystallized grainsize as a paleopiezometer in quartz-bearing mylonite zones. *Tectonophysics* **78,** 475–508.

Fleitout, L. and Froidevaux, C. (1980). Thermal and mechanical evolution of shear zones. *J. Struct. Geol.* **2,** 159–164.

Gittus, J.H. (1978). High-temperature deformation of two phase structures. *Phil. Trans. R. Soc. Lond. A* **288,** 121–146.

Griggs, D.T. (1967). A model of hydrolytic weakening in quartz and other silicates. *Geophys. J.R. astr. Soc.* **14,** 19–31.

Guillope, M. and Poirier, J.P. (1979). Dynamic recrystallization during creep of single-crystalline halite: An experimental study. *J. Geoph. Res.* **84,** 5557–5567.

Heard, J.C. (1963). Effects of large changes in strain rate in the experimental deformation of Yule marble. *J. Geol.* **71,** 162–195.

Heard, H.C. (1972). Steady-state flow in polycrystalline halite at pressure of 2 kilobars. *Amer. Geophys. Un. Mono.* **16,** 191–209.

Heard, H.C. (1976). Comparison of the flow properties of rocks at crustal conditions. *Phil. Trans. R. Soc. Lond. A* **283,** 173–186.

Heard, H.C. and Raleigh, C.B. (1972). Steady-state flow in marble at 500–800°C. *Geol. Soc. Am. Bull.* **83,** 935–956.
Higgins, M.W. (1971). Cataclastic rocks, *U.S. geol. Surv.* **687,** 1–97.
Hobbs, B.E. (1968). Recrystallization of single crystals of quartz. *Tectonophysics* **6,** 353–401.
Hubbert, M.K. and Rubey, W.W. (1959). Role of fluid pressure in mechanism of overthrust faulting. *Geol. Soc. Am. Bull* **70,** 115–166.
Kern, H., (1971). Dreiaxiale Verformungen an Solnhefener Kalkstein im Temperaturbereich von 20–650°C. Röntgengraphische Gefügeuntersuchungen mit dem Texturgoniometer. *Contr. Mineral. Petrol.* **31,** 39–66.
Kirby, S.H. and Green, H.W. (1980). Dunite xenoliths from Hualalai volcano: Evidence for mantle diapiric flow beneath the island of Hawaii. *Am. J. Science* **280–A,** 550–575.
Lister, G.S. (1978). Texture transitions in plastically deformed calcite rocks. Proc. 5th Int. Conf. on Textures of Materials, Aachen, Springer Verlag, Berlin, 199–210.
Lister, G.S. and Hobbs, B.E. (1980). The simulation of fabric development during plastic deformation and its application to quartzite: the influence of deformation history. *J. Structural Geology* **2/3,** 355–370.
Lister, G.S. and Paterson, M.S. (1979). The simulation of fabric development during plastic deformation and its application to quartzite: fabric transitions. *J. Structural Geology* **1/2,** 99–115.
Lister, G.S., Paterson, M.S. and Hobbs, B.E. (1978). The simulation of fabric development in plastic deformation and its application to quartzite: The model. *Tectonophysics* **45,** 107–158.
March, A. (1932). Mathematische Theorie der Regelung nach der Korngestalt bei affiner Deformation. *Zeitschr. Krist.* **81,** 285–298.
Mercier, J.C.C., Anderson, D.A. and Carter, N.L. (1977). Stress in the lithosphere: inferences from steady state flow of rocks. *Pure Appl. Geophys.* **115** (1/2), 199–226.
Milnes, A.G. and Pfiffner, O.A. (1977). Structural development of the Infrahelvetic complex, eastern Switzerland. *Eclogae geol. Helv.* **70,** 83–95.
Müller, W.H. and Briegel, U. (1980). Mechanical aspects of the Jura overthrust. *Eclogae geol. Helv* **73/1,** 239–250.
Müller, W.H. and Hsü, K.J. (1980). Stress distribution in overthrusting slabs and mechanics of Jura deformation. *Rock Mechanics, Suppl.* **9,** 219–232.
Müller, W.H., Schmid, S.M. and Briegel, U. (1981). Deformation experiments on anhydrite rocks of different grain sizes. Rheology and microfabric. *Tectonophysics* **78,** 527–544.
Nicolas, A. and Poirier, J.P. (1976). "Crystalline plasticity and solid state flow in metamorphic rocks". John Wiley, London, 444 pp.
Olsson, W.A. (1974). Grain size dependence of yield stress in marble. *J. Geoph. Res.* **79,** 4859–4862.
Parrish, D.K., Krivz, A. and Carter, N.L. (1976). Finite element folds of similar geometry. *Tectonophysics* **32,** 183–207.
Paterson, M.S. (1969). The ductility of rocks. *In* "Physics of Strength and Plasticity" (A.S. Argon, ed.). The M.I.T. Press, Cambridge, Mass., pp. 377–392.
Paterson, M.S. (1976). Some current aspects of experimental rock deformation. *Phil. Trans. R. Soc. Lond. A* **283,** 163–172.
Paterson, M.S. (1978). "Experimental rock deformation. The brittle field. Minerals and Rocks", Vol. 13 (P.J. Wyllie, ed.). Springer Verlag, Berlin.
Paterson, M.S. and Kekulawala, K.R.S.S. (1979). The role of water in quartz deformation. *Bull. Minéral.* **102,** 92–98.
Poirier, J.P. (1976). Plasticité à haute température des solides cristallins. Editions Eyrolles, Paris.
Poirier, J.P. (1980). Shear localization and shear instability in materials in the ductile field. *J. Structural Geology* **2,** 135–142.
Poirier, J.P. and Guillopé, M. (1979), Deformation induced recrystallization of minerals. Bull. Minéral. **102,** 67–74.
Poirier, J.P. and Nicolas, A. (1975). Deformation induced recrystallization due to progressive misorientation of subgrains, with special reference to mantle peridotites. *J. Geol.* **83,** 707–720.
Post, R.L. (1973). The flow laws of Mt. Burnet Dunite. PhD-thesis, University of California, Los Angeles.
Post, R.L. (1977). High temprature creep of Mt. Durnet Dunite. *Tectonophysics* **42,** 75–110.
Ramsay, J.G. (1980). Shear zone geometry: a review. *J. Structural Geology* **2,** 83–99.
Ross, J.V., AveLallement, H.G. and Carter, N.L. (1980). Stress dependence of recrystallized-grain and subgrain size in olivine. *Tectonophysics* **70,** 39–61.
Rutter, E.H. (1974). The influence of temperature, strain rate and interstitial water in the experimental deformation of calcite rocks. *Tectonophysics* **22,** 311–334.
Rutter, E.H. (1976). The kinetics of rock deformation by pressure solution. *Phil. Trans. R. Soc. Lond. A* **283,** 219.
Schmid, S.M. (1975). The Glarus overthrust: Field evidence and mechanical model. *Eclogae geol. Helv.* **68,** 247–280.
Schmid, S.M., Boland, J.N. and Paterson, M.S. (1977). Superplastic flow in finegrained limestone. *Tectonophysics* **43,** 257–291.
Schmid, S.M., Paterson, M.S. and Boland, J.N. (1980). High temperature flow and dynamic recrystallization in Carrara marble. *Tectonophysics* **65,** 245–280.
Schmid, S.M., Casey M. and Starkey, J. (1981a). The microfabric of calcite tectonites from the Helvetic nappes (Swiss Alps). *In* "Thrust and Nappe Tectonics" (K.R. McClay and N.J. Price, eds). *Geol. Soc. Spec. Publ.* **9,** 151–158.
Schmid, S.M., Casey, M. and Starkey, J. (1981b). An illustration of the advantages of a complete texture analysis described by the orientation distribution function (ODF) using quartz pole figure data. *Tectonophysics* **78,** 101–118.
Sellars, C.M. (1977). Recrystallization of metals during hot deformation. *Phil. Trans. R. Soc. Lond. A* **288,** 147–158.
Simpson, C. (1980). Oblique girdle orientation patterns of quartz c-axes from a shear zone in the basement core of the Maggia Nappe Ticino, Switzerland, *J. Structural Geology* **2,** 243–247.
Spang, J.H. and Brown, S.P. (1981). Dynamic analysis of a small imbricate thrust. *In* "Thrust and Nappe Tectonics" (K.R. McClay and N.J. Price, eds). *Geol. Soc. Spec. Publ.* **9,** 143–149.
Tullis, J.A. (1979). High temperature deformation of rocks and minerals. *Rev. Geophys. Space Phys.* **17,** 1137–1154.
Tullis, J., Shelton, G.L. and Yund, R.A. (1979). Pressure dependence of rock strength: implication for hydrolytic weakening. *Bull. Minéral* **102,** 110–114.
Turner, F.J. and Weiss, L.E. (1963). "Structural Analysis of Metamorphic Tectonites". McGraw Hill, New York, 545 pp.
Twiss, R.J. (1966). Structural superplastic creep and linear viscosity in the Earth's mantle. *Earth Plan. Sci. lett.* **33,** 86–100.
Twiss, R.J. (1977). Theory and applicability of a recrystallized grain size paleopiezometer. *In* "Stress in the Earth" (M. Wyss, ed.). Reprint from *Pageoph.* **115,** in CCRG, 3, Birkhäuser Verlag, Basel, pp. 227–244.
Weertman, J. (1968). Dislocation climb theory of steady state creep. *Trans. ASM* **61,** 681–694.
White, S.H. (1979). Difficulties associated with paleostress estimates. *Bull. Minéral.* **102,** 210–215.
White, S.H., Burrows, S.E., Carreras, J., Shaw, N.D. and Humphreys, F.J. (1980). On mylonites in ductile shear zones. *J. Structural Geology* **2,** 175–187.